

Determination of Klinkenberg and higher-order correction tensors for slip flow in porous media

Didier Lasseux 

*Université Bordeaux, Centre National de la Recherche Scientifique, Bordeaux INP,
I2M, UMR 5295, F-33400 Talence, France*

Tony Zaouter

CEA, DES, ISEC, DPME, SEME, Laboratoire d'Étanchéité, Université Montpellier, Marcoule 30207, France

Francisco J. Valdés-Parada 

*División de Ciencias Básicas e Ingeniería, Universidad Autónoma Metropolitana-Iztapalapa,
Avenida Ferrocarril San Rafael Atlixco, Número 186, Iztapalapa C.P. 09310, CDMX, Mexico*



(Received 29 January 2023; accepted 25 April 2023; published 10 May 2023)

An efficient method is reported to determine correction tensors at successive orders in the Knudsen number (i.e., the Klinkenberg and higher corrections) to approximate the apparent permeability tensor characterizing one-phase, creeping, Newtonian, isothermal slip flow in homogeneous porous media. It is shown that the Klinkenberg correction tensor can be obtained from the solution of the same ancillary (closure) problem that is required to compute the intrinsic permeability tensor. More generally, correction tensors up to the $(2M - 1)$ th order are shown to be obtained from the solution of the first M closure problems, instead of the $2M$ ones suggested by the upscaling procedure and associated closure scheme. Moreover, it is demonstrated that all the correction tensors are symmetric, the odd and even order ones being respectively positive and negative. In particular, this indicates that the apparent permeability tensor at the first order in the Knudsen number is symmetric positive. The model is validated by analytical solutions in the simple cases of flow in parallel plates and bundle of parallel cylindrical tubes and by numerical simulations performed in a model two-dimensional structure. An improvement in the apparent permeability prediction is shown using a Padé approximant.

DOI: [10.1103/PhysRevFluids.8.053401](https://doi.org/10.1103/PhysRevFluids.8.053401)

I. INTRODUCTION

Gas slip flow in porous media, resulting from rarefaction effects, is encountered in a wide variety of domains including gas storage in (or extraction from) geological reservoirs [1], chemical engineering processes like composite material manufacturing by chemical vapor infiltration [2], filtration and separation, and gas flow in nanoporous rocks [3], to cite only a few. The slip flow regime, characteristic of a Knudsen number (defined as the mean free path to pore-size ratio) approximately smaller than 0.1, can be modeled at the pore scale, by the Navier-Stokes (or Stokes) equations and a first-order slip boundary condition at the pore walls [4]. Nevertheless, in practice, macroscopic models are preferred in many circumstances. A widely used macroscopic equation for momentum transport is the empirical Darcy-Klinkenberg law (see, for instance, [5]).

*iqfv@xanum.uam.mx

A formal derivation of the macroscopic model was reported recently, showing that the momentum equation has a Darcy structure involving an apparent permeability tensor that can be expanded under the form of a combination of the intrinsic permeability tensor and a series of slip correction tensors at successive orders in the Knudsen number. All the tensors of interest are obtained from the solution of ancillary closure problems on a (periodic) unit cell representative of the process. In practice, solution of the closure problems for the intrinsic permeability and slip correction tensors can be computationally costly. In addition, the coupling of the successive closure problems is prone to error propagation and uncontrollable inaccuracy while increasing the order of estimation. Moreover, the convergence (when it exists) of the correction series is slow and alternate. A procedure that significantly simplifies the determination of these effective coefficients and improves convergence is therefore of utmost interest. With this purpose in mind, an expression of the j th-order slip correction tensor is derived in this paper using Green's formula. In addition, the power-series expansions are reformulated to produce the simplest Padé approximant. Although the analysis is based on gas slip flow resulting from rarefaction effects, it can be extended to situations in which slip effects are caused by other physical mechanisms (for example by the use of effective boundary conditions for flow over rough surfaces). The same type of approach to simplify the determination of the effective medium coefficients may also be envisaged for other types of transport phenomena.

The presentation is organized as follows. In Sec. II, the macroscopic model and associated closure problems are recalled. A procedure is developed in Sec. III, showing that the solution of the first M closure problems (instead of $2M$ as implied so far) is only required to obtain the correction tensors up to the $(2M - 1)$ th order. It is also proved in this section that all the correction tensors are symmetric and positive (respectively for the odd order) and negative (respectively for the even order). In particular, it shows that the first-order Klinkenberg slip correction tensor can be obtained from the solution of the same closure problem that provides the intrinsic permeability tensor and that the apparent permeability tensor at this first order of approximation is symmetric positive. In Sec. IV, a Padé approximant is proposed for the prediction of the apparent permeability tensor. The overall improvements are validated in Sec. V through analytical solutions in simple configurations and numerical simulations in a model two-dimensional (2D) periodic structure. Conclusions are drawn in Sec. VI.

II. MACROSCOPIC MODEL FOR ONE-PHASE SLIP FLOW IN POROUS MEDIA

A. Upscaled balance equation

Consider the slightly compressible, Newtonian, isothermal, creeping slip flow of a single fluid (the β phase) characterized by its density, ρ , dynamic viscosity, μ , pressure, p , and velocity, \mathbf{v} , in a rigid and homogeneous porous medium, of characteristic length L , as the one sketched in Fig. 1(a). For this system, let ℓ_σ and ℓ_β be the characteristic length scales respectively associated to the solid phase (i.e., the σ phase) and fluid phase in the porous medium bulk. The flow description at the macroscale requires defining an averaging domain \mathcal{V} , of measure V , which is representative as long as its characteristic size, r_0 , is constrained by $\max(\ell_\beta, \ell_\sigma) \ll r_0 \ll \min(L)$. Over this averaging domain, let $\langle \psi \rangle$ and $\langle \psi \rangle^\beta$ represent the superficial and intrinsic averages of a pore-scale quantity ψ , respectively defined as

$$\langle \psi \rangle = \frac{1}{V} \int_{\mathcal{V}} \psi \, dV, \quad \langle \psi \rangle^\beta = \frac{1}{V_\beta} \int_{\mathcal{V}_\beta} \psi \, dV, \quad (1)$$

where \mathcal{V}_β (of measure V_β) is the portion of \mathcal{V} occupied by the fluid phase. Note that $\langle \psi \rangle = \varepsilon \langle \psi \rangle^\beta$, where $\varepsilon = V_\beta/V$ is the porosity of the porous medium.

Using these definitions, the macroscopic model for the flow under consideration was formally derived in previous works by upscaling the governing equations at the pore scale [6,7]. It is

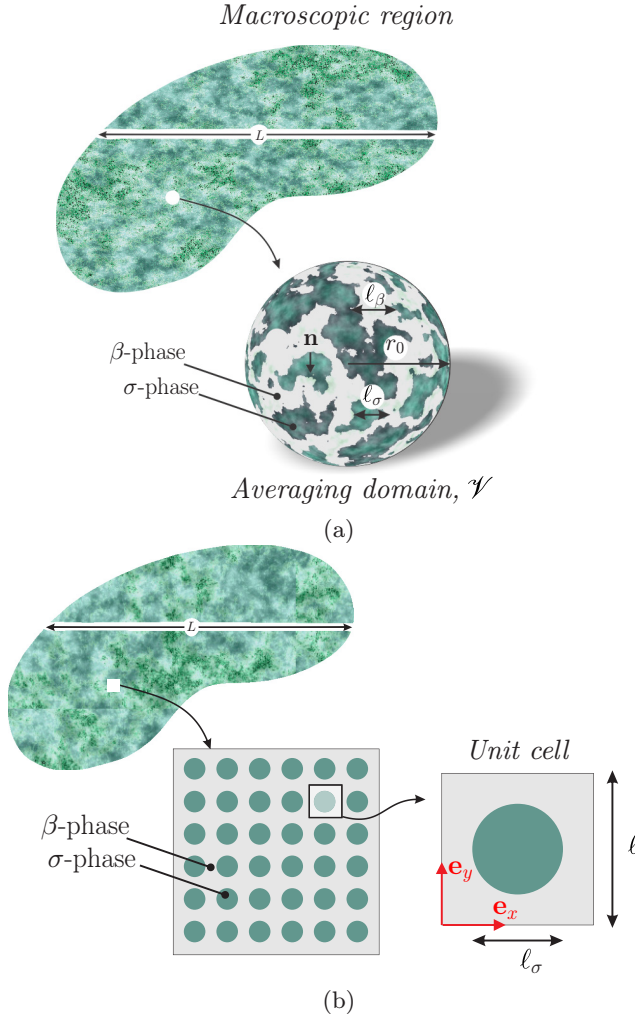


FIG. 1. (a) Sketch of a porous medium and an averaging domain \mathcal{V} for single-phase flow, including the characteristic length scales associated to the macroscale (L) and microscale (ℓ_σ and ℓ_β). (b) Example of a periodic unit cell for a model representation of the solid skeleton as an array of inline cylinders of circular cross section.

given by

$$\frac{\partial \langle \rho \rangle^\beta}{\partial t} + \nabla \cdot (\varepsilon^{-1} \langle \rho \rangle^\beta \langle \mathbf{v} \rangle) = 0, \quad (2a)$$

$$\begin{aligned} \langle \mathbf{v} \rangle &= -\frac{\mathbf{K}_s}{\mu} \cdot \nabla \langle p \rangle^\beta \simeq -\frac{\widehat{\mathbf{K}}_m}{\mu} \cdot \nabla \langle p \rangle^\beta \\ &= -\frac{\mathbf{K}}{\mu} \cdot \left(\mathbf{I} + \sum_{j=1}^m (\xi \bar{\lambda})^j \mathbf{S}_j \right) \cdot \nabla \langle p \rangle^\beta. \end{aligned} \quad (2b)$$

In addition, the macroscopic state equation can be written as

$$\langle \rho \rangle^\beta = F(\langle p \rangle^\beta), \quad (2c)$$

where F represents the functional dependence of $\langle \rho \rangle^\beta$ on $\langle p \rangle^\beta$ in accordance with the hypothesis of a barotropic fluid. In Eq. (2b), ξ is a parameter associated to the reflection process at the solid-fluid interfaces, $\mathcal{A}_{\beta\sigma}$, $\xi = \frac{2-\sigma_v}{\sigma_v}$, where σ_v is the tangential momentum accommodation coefficient ($\sigma_v = 1$ for a perfectly diffuse reflection). In addition, $\bar{\lambda}$ is the average mean-free path in the fluid at the average pressure and temperature that depends on $1/\langle \rho \rangle^\beta$ [see Eq. (2.15) in [7]]. Moreover, \mathbf{K}_s and \mathbf{K} are, respectively, the slip corrected apparent permeability and intrinsic permeability second-order tensors, that have been shown to be symmetric and positive [see [8] (Sec. 3.3 p.12 and Appendix C) for \mathbf{K}_s and [9] and Sec. 3.3 in [10] for \mathbf{K}]. Finally, $(\xi\bar{\lambda})^j \mathbf{S}_j$ is the j th – order slip correction (second-rank) tensor and \mathbf{I} is the identity tensor. In addition, in Eq. (2b),

$$\widehat{\mathbf{K}}_m = \mathbf{K} \cdot \left(\mathbf{I} + \sum_{j=1}^m (\xi\bar{\lambda})^j \mathbf{S}_j \right) \quad (3)$$

is the m th-order approximation in $\xi\bar{\text{Kn}} = \xi\bar{\lambda}/\ell_\beta$ ($\bar{\text{Kn}}$ is the Knudsen number) of \mathbf{K}_s . This approximation is obtained from a Maclaurin series expansion in $\xi\bar{\text{Kn}}$ (see Sec. 4.1 in [7]) of the closure problem yielding \mathbf{K}_s [see Eqs. (3.7) in this reference]. This assumes $\xi\bar{\text{Kn}} < 1$, consistent with the slip condition that requires $\xi\bar{\text{Kn}} \lesssim 0.1$. Conversely to \mathbf{K}_s , that is not intrinsic and has to be computed at any value of $\xi\bar{\text{Kn}}$, $\widehat{\mathbf{K}}_m$ only involves intrinsic quantities, and is hence fully predictive. Note that the above macroscopic slip flow model, presented in the framework of rarefied gas flow, can be generalized to other flow situations for which a first-order slip boundary condition may be applied at solid-fluid interfaces at the pore scale. This is the case, for instance, when an effective boundary condition is used to model viscous flow over rough surfaces [11,12]. Results reported below can hence be generalized to any of these situations while considering $\xi\bar{\lambda}$ as the slip length.

B. Closure problems

The second-order tensors \mathbf{K} and \mathbf{S}_j present in the average momentum equation are obtained from the solution of the associated intrinsic closure problems that are defined in a periodic unit cell representative of the system, such as that sketched in Fig. 1(b). In space of dimension N ($N = 2, 3$), they are given by (see Sec. 4.1 in [7]),

$$\text{0th order} \quad \nabla \cdot \mathbf{D}_0 = \mathbf{0}, \quad \text{in } \mathcal{V}_\beta, \quad (4a)$$

$$\mathbf{0} = \nabla \cdot \mathbf{T}_{\mathbf{d}_0} + \mathbf{I}, \quad \text{in } \mathcal{V}_\beta, \quad (4b)$$

$$\mathbf{D}_0 = \mathbf{0}, \quad \text{at } \mathcal{A}_{\beta\sigma}, \quad (4c)$$

$$\langle \mathbf{d}_0 \rangle^\beta = \mathbf{0}, \quad (4d)$$

$$\text{with periodicity } \boldsymbol{\psi}(\mathbf{r} + \mathbf{l}_i) = \boldsymbol{\psi}(\mathbf{r}), \quad \boldsymbol{\psi} = \mathbf{D}_0, \quad \mathbf{d}_0, \quad i = 1, \dots, N, \quad (4e)$$

$$\langle \mathbf{D}_0 \rangle = \mathbf{K}. \quad (4f)$$

$$\text{jth order, } j = 1, \dots, m, \quad \nabla \cdot \mathbf{D}_j = \mathbf{0}, \quad \text{in } \mathcal{V}_\beta, \quad (5a)$$

$$\mathbf{0} = \nabla \cdot \mathbf{T}_{\mathbf{d}_j}, \quad \text{in } \mathcal{V}_\beta, \quad (5b)$$

$$\mathbf{D}_j = -\mathbf{P} \cdot (\mathbf{n} \cdot \mathbf{T}_{\mathbf{d}_{j-1}}), \quad \text{at } \mathcal{A}_{\beta\sigma}, \quad (5c)$$

$$\langle \mathbf{d}_j \rangle^\beta = \mathbf{0}, \quad (5d)$$

$$\text{with periodicity } \boldsymbol{\psi}(\mathbf{r} + \mathbf{l}_i) = \boldsymbol{\psi}(\mathbf{r}), \quad \boldsymbol{\psi} = \mathbf{D}_j, \quad \mathbf{d}_j, \quad i = 1, \dots, N, \quad (5e)$$

$$\langle \mathbf{D}_j \rangle = \mathbf{K} \cdot \mathbf{S}_j. \quad (5f)$$

In the above equations, \mathbf{l}_i represents the periodic lattice vector in the i th direction, whereas $\mathbf{T}_{\mathbf{d}_l}$ denotes a stresslike third-order tensor defined as

$$\mathbf{T}_{\mathbf{d}_l} = -\mathbf{I}\mathbf{d}_l + \nabla\mathbf{D}_l + (\nabla\mathbf{D}_l)^{T1}, \quad l = 0, \dots, m. \quad (6)$$

The vector \mathbf{d}_l and second-order tensor \mathbf{D}_l are the closure variables at the l th order. Moreover, $T1$ is used for the transpose of a third-order tensor, \mathbf{M} , that permutes the two first indices, i.e., $M_{ijk}^{T1} = M_{jik}$, M_{ijk} being the ijk component of \mathbf{M} . In Eq. (5c), $\mathbf{P} = \mathbf{I} - \mathbf{n}\mathbf{n}$ is the local projection tensor onto $\mathcal{A}_{\beta\sigma}$, \mathbf{n} being the unit normal vector at $\mathcal{A}_{\beta\sigma}$, taken as that pointing out of \mathcal{V}_β in the following. Note that the first-order slip boundary condition at $\mathcal{A}_{\beta\sigma}$ was originally expressed as $\mathbf{D}_j = -\mathbf{P} \cdot \{\mathbf{n} \cdot [\nabla\mathbf{D}_{j-1} + (\nabla\mathbf{D}_{j-1})^{T1}]\}$ [see Eq. (4.7) in [7]]. However, $\mathbf{P} \cdot [\mathbf{n} \cdot (-\mathbf{I}\mathbf{d}_{j-1})] = -(\mathbf{P} \cdot \mathbf{n})\mathbf{d}_{j-1} = \mathbf{0}$ due to the property of the projection tensor \mathbf{P} , leading to the boundary condition written in the compact form of Eq. (5c).

Clearly, the determination of the j th-order slip correction tensor requires the solution of all the closure problems up to this order. All of them have an equivalent complexity and are sequentially coupled through the slip boundary condition at $\mathcal{A}_{\beta\sigma}$. Since the j th order closure problem involves spatial derivatives of \mathbf{D}_{j-1} , inaccuracy of the numerical simulations strongly increases with j due to propagation of numerical errors. Therefore, any simplification of the computational procedure from this regard is of major interest.

For a sufficiently small value of $\overline{\mathbf{K}\mathbf{n}}$, $\widehat{\mathbf{K}}_1$ is a reasonable approximation of \mathbf{K}_s and the average momentum equation can be written as

$$\langle \mathbf{v} \rangle \simeq -\frac{\widehat{\mathbf{K}}_1}{\mu} \cdot \nabla \langle p \rangle^\beta = -\frac{\mathbf{K}}{\mu} \cdot (\mathbf{I} + \xi \bar{\lambda} \mathbf{S}_1) \cdot \nabla \langle p \rangle^\beta, \quad (7)$$

that is the commonly used macroscopic model for slip flow in porous media. Indeed, for conditions in which the ideal gas law is applicable, the above equation coincides with the Klinkenberg model [13], written in its tensorial form (see discussion in Sec. VIA in [6]). Nevertheless, in some circumstances, $\widehat{\mathbf{K}}_m$ with $m > 1$ is a much better approximation of \mathbf{K}_s . This is highlighted in [7] and illustrated in Sec. VB.

Progress towards important simplifications of the computation of the slip correction tensors $(\xi \bar{\lambda})^j \mathbf{S}_j$ is achieved by deriving an alternative expression of $\langle \mathbf{D}_j \rangle$ given in Eq. (5f) as described below.

III. ALTERNATIVE EXPRESSION OF THE j th-ORDER SLIP CORRECTION

The procedure starts by considering the following Green's formula, valid for any two arbitrary vector fields \mathbf{a} and \mathbf{b} , and second-order solenoidal tensor fields \mathbf{A} and \mathbf{B} , that is given by (see the derivation in Appendix A in [14])

$$\int_{\mathcal{V}_\beta} [\mathbf{A}^T \cdot (\nabla \cdot \mathbf{T}_b) - (\nabla \cdot \mathbf{T}_a)^T \cdot \mathbf{B}] dV = \int_{\mathcal{A}_\beta} [\mathbf{A}^T \cdot (\mathbf{n} \cdot \mathbf{T}_b) - (\mathbf{n} \cdot \mathbf{T}_a)^T \cdot \mathbf{B}] dA. \quad (8a)$$

Here, \mathcal{A}_β denotes the surfaces enclosing \mathcal{V}_β that are composed of $\mathcal{A}_{\beta\sigma}$ and the entrances and exits, $\mathcal{A}_{\beta e}$, of the β phase at the unit cell edges (i.e., $\mathcal{A}_\beta = \mathcal{A}_{\beta\sigma} \cup \mathcal{A}_{\beta e}$), whereas

$$\mathbf{T}_a = -\mathbf{I}\mathbf{a} + \nabla\mathbf{A} + \nabla\mathbf{A}^{T1}, \quad \mathbf{T}_b = -\mathbf{I}\mathbf{b} + \nabla\mathbf{B} + \nabla\mathbf{B}^{T1}. \quad (8b)$$

Taking $\mathbf{a} \equiv \mathbf{d}_0$, $\mathbf{A} \equiv \mathbf{D}_0$, $\mathbf{b} \equiv \mathbf{d}_j$, and $\mathbf{B} \equiv \mathbf{D}_j$ in this formula, making use of Eqs. (4b) and (5b), together with the boundary condition given in Eq. (4c), as well as periodicity, and dividing the result by V , leads to ($j = 1, \dots, m$)

$$\langle \mathbf{D}_j \rangle = -\frac{1}{V} \int_{\mathcal{A}_{\beta\sigma}} (\mathbf{n} \cdot \mathbf{T}_{\mathbf{d}_0})^T \cdot \mathbf{D}_j dA. \quad (9)$$

Note that in this expression, the area integral reduces to $\mathcal{A}_{\beta\sigma}$ as that over $\mathcal{A}_{\beta e}$ cancels out due to periodicity of the closure variables. The boundary condition given in Eq. (5c) can now be taken into account to rewrite this last relationship as

$$\langle \mathbf{D}_j \rangle = \frac{1}{V} \int_{\mathcal{A}_{\beta\sigma}} (\mathbf{n} \cdot \mathbf{T}_{\mathbf{d}_0})^T \cdot \mathbf{P} \cdot (\mathbf{n} \cdot \mathbf{T}_{\mathbf{d}_{j-1}}) dA, \quad (10)$$

where $\mathbf{T}_{\mathbf{d}_l}$ ($l = 0, \dots, j-1$) is defined in Eq. (6).

If one is only interested in the first-order (Klinkenberg) correction, the procedure stops at the level of Eq. (10), which, for $j = 1$, gives

$$\langle \mathbf{D}_1 \rangle = \frac{1}{V} \int_{\mathcal{A}_{\beta\sigma}} (\mathbf{n} \cdot \mathbf{T}_{\mathbf{d}_0})^T \cdot \mathbf{P} \cdot (\mathbf{n} \cdot \mathbf{T}_{\mathbf{d}_0}) dA. \quad (11)$$

For $j \geq 2$, the procedure is continued by first substituting the transpose of the slip boundary condition given in Eq. (5c) (taking $j = 1$ in this equation) into Eq. (10). Since \mathbf{P} is a symmetric tensor, this yields

$$\langle \mathbf{D}_j \rangle = -\frac{1}{V} \int_{\mathcal{A}_{\beta\sigma}} \mathbf{D}_1^T \cdot (\mathbf{n} \cdot \mathbf{T}_{\mathbf{d}_{j-1}}) dA. \quad (12)$$

Second, let Green's formula given in Eq. (8a) be considered again with $\mathbf{a} \equiv \mathbf{d}_1$, $\mathbf{A} \equiv \mathbf{D}_1$, $\mathbf{b} \equiv \mathbf{d}_{j-1}$, and $\mathbf{B} \equiv \mathbf{D}_{j-1}$. Since $\mathbf{T}_{\mathbf{d}_1}$ and $\mathbf{T}_{\mathbf{d}_{j-1}}$ are both solenoidal, and taking into account periodicity, this leads to

$$\int_{\mathcal{A}_{\beta\sigma}} \mathbf{D}_1^T \cdot (\mathbf{n} \cdot \mathbf{T}_{\mathbf{d}_{j-1}}) dA = \int_{\mathcal{A}_{\beta\sigma}} (\mathbf{n} \cdot \mathbf{T}_{\mathbf{d}_1})^T \cdot \mathbf{D}_{j-1} dA, \quad (13)$$

which, once substituted back into Eq. (12), gives

$$\langle \mathbf{D}_j \rangle = -\frac{1}{V} \int_{\mathcal{A}_{\beta\sigma}} (\mathbf{n} \cdot \mathbf{T}_{\mathbf{d}_1})^T \cdot \mathbf{D}_{j-1} dA. \quad (14)$$

Comparison of Eqs. (9) and (14) indicates that the first and second terms under the area integral in the latter have been respectively increased and decreased by one order. Consequently, the above two steps can be repeated recurrently until reaching the following expressions ($j \geq 1$):

$$\langle \mathbf{D}_j \rangle = -\frac{1}{V} \int_{\mathcal{A}_{\beta\sigma}} (\mathbf{n} \cdot \mathbf{T}_{\mathbf{d}_{j/2}})^T \cdot \mathbf{D}_{j/2} dA, = \frac{1}{V} \int_{\mathcal{A}_{\beta\sigma}} (\mathbf{n} \cdot \mathbf{T}_{\mathbf{d}_{j/2}})^T \cdot \mathbf{P} \cdot (\mathbf{n} \cdot \mathbf{T}_{\mathbf{d}_{j/2-1}}) dA, \quad j \text{ even}, \quad (15a)$$

and

$$\langle \mathbf{D}_j \rangle = \frac{1}{V} \int_{\mathcal{A}_{\beta\sigma}} (\mathbf{n} \cdot \mathbf{T}_{\mathbf{d}_{(j-1)/2}})^T \cdot \mathbf{P} \cdot (\mathbf{n} \cdot \mathbf{T}_{\mathbf{d}_{(j-1)/2}}) dA, \quad j \text{ odd}. \quad (15b)$$

Note that Eq. (15b) is indeed valid for $j = 1$ as it coincides with Eq. (11) in that case.

The above expressions show that the slip correction tensors up to the order $2M - 1$ (and, therefore, $\widehat{\mathbf{K}}_{2M-1}$) are obtained from the solution of the first M closure problems, instead of requiring the first $2M$ ones as expected from the statement of the closure scheme given by Eqs. (4) and (5). This represents a considerable simplification since, in this way, the computational requirement is divided by 2, and error propagation is limited. It is worth adding that, although $\langle \mathbf{D}_j \rangle$ is still related to the spatial derivatives of $\mathbf{D}_{j/2}$ (j even) or $\mathbf{D}_{(j-1)/2}$ (j odd), this coupling is contained in an integral operator, which may smooth the numerical errors. Further properties of the correction tensors can now be derived on the basis of Eq. (15).

A. Properties of the slip correction tensors

For odd values of j , $\langle \mathbf{D}_j \rangle$ is clearly symmetric. This readily follows from its expression given in Eq. (15b) and the fact that \mathbf{P} is a symmetric tensor. Moreover, let $\boldsymbol{\omega}$ be an arbitrary nonzero constant vector and $\mathbf{M} = \mathbf{n} \cdot \mathbf{T}_{\mathbf{d}_{(j-1)/2}}$. Taking into account the fact that $\mathbf{P} = \mathbf{P} \cdot \mathbf{P}$, one can write

$$\boldsymbol{\omega} \cdot \langle \mathbf{D}_j \rangle \cdot \boldsymbol{\omega} = \frac{1}{V} \int_{\mathcal{A}_{\beta\sigma}} \boldsymbol{\omega} \cdot \mathbf{M}^T \cdot \mathbf{P} \cdot \mathbf{M} \cdot \boldsymbol{\omega} dA$$

$$\begin{aligned}
 &= \frac{1}{V} \int_{\mathcal{A}_{\beta\sigma}} [(\mathbf{M} \cdot \boldsymbol{\omega}) \cdot \mathbf{P}] \cdot [\mathbf{P} \cdot (\mathbf{M} \cdot \boldsymbol{\omega})] dA \\
 &= \frac{1}{V} \int_{\mathcal{A}_{\beta\sigma}} [(\mathbf{M} \cdot \boldsymbol{\omega}) \cdot \mathbf{P}]^2 dA.
 \end{aligned} \tag{16}$$

This proves that $\langle \mathbf{D}_j \rangle$ is positive in that case.

For even values of j , Eq. (15a) can be rewritten as $\langle \mathbf{D}_j \rangle = -\frac{1}{V} \int_{\mathcal{A}_{\beta\sigma}} (\mathbf{n} \cdot \mathbf{M})^T \cdot \mathbf{D}_{j/2} dA$, with, this time, $\mathbf{M} = \nabla \mathbf{D}_{j/2} + (\nabla \mathbf{D}_{j/2})^{T1}$. Denoting by the superscripts $T2$ and $T3$ the transposes, respectively defined by $M_{ijk}^{T2} = M_{ikj}$ and $M_{ijk}^{T3} = M_{kji}$, noticing that $(\mathbf{n} \cdot \mathbf{M})^T = \mathbf{n} \cdot \mathbf{M}^{T2}$, and by application of the divergence theorem, it follows that

$$\langle \mathbf{D}_j \rangle = -\langle \nabla \cdot (\mathbf{M}^{T2} \cdot \mathbf{D}_{j/2}) \rangle = -\langle \nabla \cdot \mathbf{M}^{T2} \cdot \mathbf{D}_{j/2} \rangle - \langle \nabla \mathbf{D}_{j/2}^{T3} : \mathbf{M} \rangle, \tag{17}$$

where $:$ is the double dot product defined in the nested convention sense. However, $\nabla \cdot \mathbf{M}^{T2} = (\nabla \cdot \mathbf{M})^T = (\nabla \mathbf{d}_{j/2})^T$, where the last part of this equality is deduced from Eq. (5b). Employing the same procedure as that developed in [9] [see Eq. (8) and associated comment therein], it follows that $\langle \nabla \cdot \mathbf{M}^{T2} \cdot \mathbf{D}_{j/2} \rangle = \mathbf{0}$. Therefore,

$$\langle \mathbf{D}_j \rangle = -\langle \nabla \mathbf{D}_{j/2}^{T3} : \mathbf{M} \rangle = -\frac{1}{2} \langle \mathbf{M}^{T3} : \mathbf{M} \rangle. \tag{18}$$

Making use of Einstein's notation, the kl component of $\langle \mathbf{D}_j \rangle$ is $\langle \mathbf{D}_j \rangle_{kl} = -\langle M_{knp}^{T3} M_{pnl} \rangle / 2 = -\langle M_{pnk} M_{pnl} \rangle / 2$, which shows that $\langle \mathbf{D}_j \rangle$ is a symmetric tensor. Finally, for any constant nonzero vector $\boldsymbol{\omega}$, $\boldsymbol{\omega} \cdot (\mathbf{M}^{T3} : \mathbf{M}) \cdot \boldsymbol{\omega} = \omega_k M_{knp}^{T3} M_{pnl} \omega_l = \omega_k M_{pnk} M_{pnl} \omega_l = (M_{pnk} \omega_k)^2$ is a positive quantity, which finally proves that $\langle \mathbf{D}_j \rangle$ is negative when j is even.

These results show that the slip correction tensors $\widehat{\mathbf{K}}_j$ form an alternate series.

B. First-order (Klinkenberg) slip flow model

The conclusions reached from the above developments shall now be emphasized in the case of the commonly used first-order (Klinkenberg) slip flow model [see Eq. (7)]. Indeed, Eq. (15b) (with $j = 1$) proves that the zeroth-order closure problem [Eq. (4)] is the only one to be solved in that case to determine both \mathbf{K} and $\mathbf{K} \cdot \mathbf{S}_1 = \langle \mathbf{D}_1 \rangle$. This represents a considerable improvement, dividing by 2 the computational procedure implied from upscaling, which suggests to solve both the zeroth-order [Eq. (4)] and first-order [Eq. (5) with $j = 1$] closure problems to obtain the two effective coefficients [7,15]. Moreover, since $\langle \mathbf{D}_1 \rangle$ is symmetric and positive, then so is the apparent permeability tensor $\widehat{\mathbf{K}}_1 = \mathbf{K} + \xi \bar{\lambda} \langle \mathbf{D}_1 \rangle$, completing the analysis reported in [8] (Sec. 3.3 p.12 and Appendix C).

IV. PADÉ APPROXIMANT

The above sign analysis suggests a poor convergence of $\widehat{\mathbf{K}}_m$ towards \mathbf{K}_s as m increases, as was confirmed by numerical simulations (see Fig. 10 in [7]). A better prediction of \mathbf{K}_s for a finite value of m shall be proposed with a Padé approximant, $\tilde{\mathbf{K}}_{(n,n)}$ ($n \geq 1$) given by [16]

$$\tilde{\mathbf{K}}_{(n,n)} = \left(\sum_{i=0}^n (\xi \bar{\lambda})^i \mathbf{G}_i \right) \cdot \left(\sum_{l=0}^n (\xi \bar{\lambda})^l \mathbf{F}_l \right)^{-1}, \tag{19}$$

where \mathbf{F}_l , $l = 0, \dots, n$, and \mathbf{G}_i , $i = 0, \dots, n$, are two series of second-order tensors to be identified from $\widehat{\mathbf{K}}_{2n}$. The above form is chosen so as to reproduce the expected constant behavior (when the pore-scale flow is not rectilinear) of \mathbf{K}_s in $\xi \bar{\lambda}$ in the asymptotic mathematical limit $\xi \bar{\lambda} \rightarrow +\infty$. In fact, under this perfect slip condition, it is required that the sliplike boundary condition in the closure problem defining \mathbf{K}_s [see Eq. (3.7c) in [7]] adopts a zero shearlike form. The closure problem statement with this boundary condition yields the asymptotic value of \mathbf{K}_s in this limit, except when flow is one dimensional, as in the cases explored in Sec. VA for which \mathbf{K}_s keeps a

linear dependence in the perfect slip limit. Therefore, the form of the Padé approximant proposed in Eq. (19) conveniently reproduces the asymptotic constant behavior.

For the sake of conciseness, the Padé approximant is now detailed for $n = 1$, which is the simplest one and that is expected to provide enough accuracy in the context of slip flow, i.e., $\xi \bar{K}n \lesssim 0.1$. The determination of \mathbf{F}_l , $l = 0, 1$, and \mathbf{G}_i , $i = 0, 1$, is carried out by identifying $\tilde{\mathbf{K}}_{(1,1)}$ to $\hat{\mathbf{K}}_2$, yielding

$$(\mathbf{G}_0 + \xi \bar{\lambda} \mathbf{G}_1) - \mathbf{K} \cdot \mathbf{F}_0 - \xi \bar{\lambda} (\langle \mathbf{D}_1 \rangle \cdot \mathbf{F}_0 + \mathbf{K} \cdot \mathbf{F}_1) - (\xi \bar{\lambda})^2 (\langle \mathbf{D}_2 \rangle \cdot \mathbf{F}_0 + \langle \mathbf{D}_1 \rangle \cdot \mathbf{F}_1) = \mathbf{O}[(\xi \bar{\lambda})^3]. \quad (20)$$

At this point, \mathbf{F}_0 is chosen as $\mathbf{F}_0 = \mathbf{I}$ (any other choice would simply result in a rescaling). This leads to

$$\mathbf{G}_0 = \mathbf{K}, \quad (21a)$$

$$\mathbf{F}_1 = -\langle \mathbf{D}_1 \rangle^{-1} \cdot \langle \mathbf{D}_2 \rangle, \quad (21b)$$

$$\mathbf{G}_1 = \langle \mathbf{D}_1 \rangle - \mathbf{K} \cdot \langle \mathbf{D}_1 \rangle^{-1} \cdot \langle \mathbf{D}_2 \rangle \quad (21c)$$

and, therefore,

$$\tilde{\mathbf{K}}_{(1,1)} = [\mathbf{K} + \xi \bar{\lambda} (\langle \mathbf{D}_1 \rangle - \mathbf{K} \cdot \langle \mathbf{D}_1 \rangle^{-1} \cdot \langle \mathbf{D}_2 \rangle)] \cdot (\mathbf{I} - \xi \bar{\lambda} \langle \mathbf{D}_1 \rangle^{-1} \cdot \langle \mathbf{D}_2 \rangle)^{-1}. \quad (22)$$

It should be noticed that this approximant only involves \mathbf{K} , $\langle \mathbf{D}_1 \rangle$, and $\langle \mathbf{D}_2 \rangle$, which are available from the solution of only the zeroth- and first-order closure problems. The performance of this approximant is illustrated in Sec. VB.

V. VALIDATION IN SIMPLE CASES

A. Analytical solutions

To illustrate the above procedure, simple cases are now considered consisting of a set of parallel plates distant from $2h$ and a bundle of parallel cylindrical tubes of radius R , for which analytical solutions of the closure (and flow) problems are available. An orthonormal (x, y) set of Cartesian coordinates in the parallel-plates case, and one of cylindrical coordinates in the bundle of tubes case, with r the radial coordinate, are used, the x axis being along the symmetry axis of the unit cell in each case. For symmetry reasons, the solution for D_{0xx} is only required in both cases for which, in addition, $K_{sxx} = \hat{K}_{1,xx}$, i.e., the j th-order correction is zero for $j \geq 2$. Therefore, the macroscopic momentum equation reduces to the x projection of Eq. (7). The results for incompressible flow are the following.

1. Parallel plates

$D_{0xx} = (-y^2 + h^2)/2$, yielding $K_{xx} = \varepsilon h^2/2$ from Eq. (4f) and $\langle D_{1xx} \rangle = \frac{\varepsilon}{2h} [(\frac{dD_{0xx}}{dy})^2_{y=-h} + (\frac{dD_{0xx}}{dy})^2_{y=h}] = \varepsilon h$ from Eq. (15b), which exactly coincide with the result obtained from the solution of Eq. (5) for $j = 1$, that is $D_{1xx} = h$.

2. Bundle of tubes

$D_{0xx} = (-r^2 + R^2)/4$, yielding $K_{xx} = \varepsilon R^2/8$ from Eq. (4f) and $\langle D_{1xx} \rangle = \frac{\varepsilon}{\pi R^2} \int_0^{2\pi} (\frac{dD_{0xx}}{dr})^2_{r=R} R d\theta = \varepsilon R/2$ from Eq. (11). The latter is again exactly the result that follows from the solution of Eq. (5) for $j = 1$, that is given by $D_{1xx} = R/2$.

In both cases, the results on $\hat{K}_{1,xx} = K_{xx} + \xi \bar{\lambda} \langle D_{1xx} \rangle$ reported above are in agreement with K_{sxx} calculated from the average solution of the Stokes equations with a first-order slip correction at $\mathcal{A}_{\beta\sigma}$. These two examples serve as a validation of the procedure developed above to obtain the first-order slip correction from the solution of the closure problem yielding the intrinsic permeability.

TABLE I. Values of D_{jxx}^* , $j = 1, \dots, 5$, obtained from Eqs. (5f) and (15). The latter only requires the solution of Eq. (5) for j up to 2.

	Eq. (5f)	Eq. (15)	Δ (%)
$\langle D_{1xx}^* \rangle$	0.2117	0.2117	8.8×10^{-6}
$\langle D_{2xx}^* \rangle$	-1.8446	-1.8446	3.8×10^{-6}
$\langle D_{3xx}^* \rangle$	18.8594	18.8594	7.8×10^{-6}
$\langle D_{4xx}^* \rangle$	-242.6804	-242.6787	7.1×10^{-4}
$\langle D_{5xx}^* \rangle$	4272.9506	4226.5686	1.085

B. Numerical results in a simple 2D structure

To further illustrate the developments detailed above, a simple 2D structure made of a square pattern of parallel cylinders of circular cross section, as represented in Fig. 1(b) together with its unit cell, is now considered, taking $\varepsilon = 0.8$. Since the structure is orthotropic, the analysis is restricted to $K_{sxx}^* = K_{sxx}/\ell^2$, that is compared to its approximations $\widehat{K}_{mxx}^* = \widehat{K}_{mxx}/\ell^2$ ($m = 1, \dots, 5$) and the Padé approximant $\widetilde{K}_{(1,1)xx}^* = \widetilde{K}_{(1,1)xx}/\ell^2$; ℓ is the unit cell size [see Fig. 1(b)]. The permeabilities were computed from the solution of the closure problem given in Eq. (3.7) in [7] for K_{sxx}^* [see results in Fig. 10(d) in this reference], those given in Eqs. (4) and (5) for \widehat{K}_{mxx}^* , using Eqs. (5f) and (15) to obtain $\langle D_{jxx}^* \rangle = \langle D_{jxx} \rangle / \ell^{2-j}$ ($j = 1, \dots, m$) in order to compare the two procedures, and finally Eq. (22) to compute $\widetilde{K}_{(1,1)xx}^*$. All the closure problems were solved with a boundary-element method using constant elements. The dimensionless boundary-element size (taking ℓ as the reference) for these computations is $\approx 3.726 \times 10^{-4}$, which implies $\approx 15\,000$ elements on $\mathcal{A}_{\beta\sigma} \cup \mathcal{A}_{\beta e}$, ensuring mesh convergence. The value of the intrinsic permeability for this structure is found to be $K_{xx}^* \simeq 0.0194073$. The value of ℓ_β to compute $\overline{Kn} = \bar{\lambda}/\ell_\beta$ was taken as the slit aperture of a pair of parallel plates yielding the same intrinsic permeability (i.e., $\ell_\beta = \sqrt{12K_{xx}^*/\varepsilon}$).

To obtain $\langle D_{5xx}^* \rangle$ from Eq. (15b), it is only necessary to solve the first three closure problems, i.e., Eqs. (4) and (5) for j up to 2. However, to compare the values of $\langle D_{jxx}^* \rangle$, the latter were also solved up to $j = 5$. The results on $\langle D_{jxx}^* \rangle$ obtained from Eqs. (5f) and (15) are reported in Table I. As shown by the absolute values of their relative difference, Δ , taking the result from Eq. (5f) as the reference, they are in excellent agreement, as Δ remains smaller than 1.1%, although it increases significantly with the order, as expected, due to errors propagation resulting from the dependence of \mathbf{D}_j upon $\nabla \mathbf{D}_{j-1}$. This further validates the efficient procedure given by Eq. (15) to obtain $\langle \mathbf{D}_j \rangle$.

The comparison between K_{sxx}^* and its approximations \widehat{K}_{mxx}^* ($m = 1, \dots, 5$) and $\widetilde{K}_{(1,1)xx}^*$ is reported versus $\xi \overline{Kn}$ in Fig. 2 for $\xi \overline{Kn} \leq 0.1$. It can be clearly seen that the convergence of \widehat{K}_{mxx}^* is alternate and slow (a slight improvement is only achieved with the fifth order with respect to the third order), whereas the Padé approximant outperforms since its prediction of K_{sxx}^* is within less than 0.3% of error for $\xi \overline{Kn} \leq 0.1$. As a result of the development reported in this paper, this excellent approximation only requires the solution of the closure problems up to the first order. This represents a tremendous improvement as the latter would only provide \widehat{K}_{1xx}^* if the approach initially suggested by the closure scheme were followed.

VI. CONCLUSIONS

An efficient method is provided in this paper to predict the apparent permeability tensor for steady, one-phase, Newtonian, isothermal, creeping slip flow in homogeneous porous media from the intrinsic permeability and the corrections at the successive orders in the Knudsen number. It is shown that the solution of the first M closure problems, instead of $2M$ implied by the upscaling and closure procedure, is necessary to obtain the effective coefficients for the correction at the $(2M - 1)$ th order. This represents a considerable improvement as it reduces the computational effort

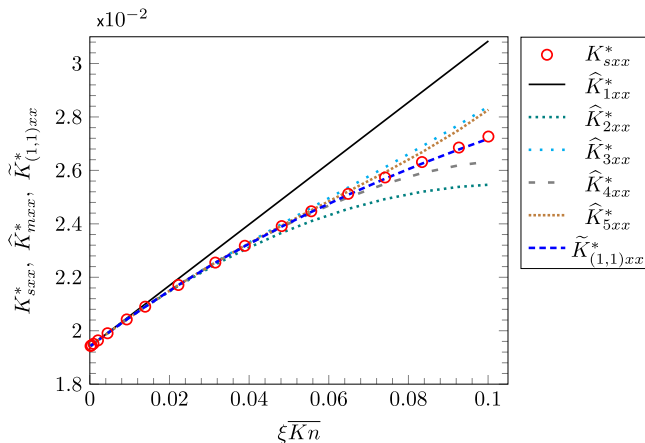


FIG. 2. Apparent slip corrected permeability, $K_{sxx}^* = K_{sxx}/\ell^2$, vs $\xi \overline{Kn}$, its approximations $\widehat{K}_{mxx}^* = \widehat{K}_{mxx}/\ell^2$ ($m = 1, \dots, 5$), and the Padé approximant $\widetilde{K}_{(1,1)xx}^* = \widetilde{K}_{(1,1)xx}/\ell^2$. The results correspond to the unit cell represented in Fig. 1(b) for $\varepsilon = 0.8$.

by 2 and limits the numerical error propagation. In particular, the solution of the classical closure problem to compute the intrinsic permeability tensor also provides the first-order (Klinkenberg) correction tensor. This is of major interest as the Darcy-Klinkenberg model is of common use in practice.

The development leading to this efficient procedure also allows demonstrating that all the slip correction tensors are symmetric, the odd ones being positive whereas the even ones are negative. This indicates that the apparent permeability at the first order in the Knudsen number is symmetric and positive. Moreover, a Padé approximant is proposed to improve the performance of the prediction of the slip corrected permeability tensor.

The efficient procedure for the correction tensors evaluation and the relevance of the Padé approximant is validated with analytical results in simple configurations and numerical simulations in a model 2D configuration. The derivations proposed in this paper may also be applied to slip flow resulting from other mechanisms than the Knudsen effects envisaged here and to other transport phenomena. These applications will be explored in future works.

ACKNOWLEDGMENTS

This work was supported by the RRI BEST-Usine du Futur of the University of Bordeaux and by the GdR HydroGEMM of CNRS. T.Z. gratefully acknowledges support from the joint CEA-TECHNETICS Group France Maestral sealing laboratory.

-
- [1] C. Liu, B. Yu, H. Zhao, Z. Hong, Z. Tian, D. Zhang, and Y. Liu, Effective stress effect and slippage effect of gas migration in deep coal reservoirs, *Int. J. Rock Mech. Min. Sci.* **155**, 105142 (2022).
 - [2] C. Charles, C. Descamps, and G. L. Vignoles, Low pressure gas transfer in fibrous media with progressive infiltration: correlation between different transfer modes, *Int. J. Heat Mass Transf.* **182**, 121954 (2022).
 - [3] S. Peng, Advanced understanding of gas flow and the Klinkenberg effect in nanoporous rocks, *J. Pet. Sci. Eng.* **206**, 109047 (2021).
 - [4] E. Lauga, M. Brenner, and H. Stone, Microfluidics: The no-slip boundary condition, in *Springer Handbook of Experimental Fluid Mechanics* (Springer-Verlag, Berlin, 2007), pp. 1219–1240.

- [5] D. Lasseux and F. J. Valdés-Parada, On the developments of Darcy's law to include inertial and slip effects, *C. R. Mec.* **345**, 660 (2017).
- [6] D. Lasseux, F. J. Valdés-Parada, J. A. Ochoa-Tapia, and B. Goyeau, A macroscopic model for slightly compressible gas slip-flow in homogeneous porous media, *Phys. Fluids* **26**, 053102 (2014).
- [7] D. Lasseux, F. J. Valdés-Parada, and M. L. Porter, An improved macroscale model for gas slip flow in porous media, *J. Fluid Mech.* **805**, 118 (2016).
- [8] D. Lasseux, F. J. Valdés-Parada, and A. Bottaro, Upscaled model for unsteady slip flow in porous media, *J. Fluid Mech.* **923**, A37 (2021).
- [9] D. Lasseux and F. J. Valdés-Parada, Symmetry properties of macroscopic transport coefficients in porous media, *Phys. Fluids* **29**, 043303 (2017).
- [10] D. Lasseux, F. J. Valdés-Parada, and F. Bellet, Macroscopic model for unsteady flow in porous media, *J. Fluid Mech.* **862**, 283 (2019).
- [11] S. J. Bolaños and B. Vernescu, Derivation of the Navier slip and slip length for viscous flows over a rough boundary, *Phys. Fluids* **29**, 057103 (2017).
- [12] S. Perez, P. Moonen, and P. Poncet, On the deviation of computed permeability induced by unresolved morphological features of the pore space, *Transp. Porous Media* **141**, 151 (2022).
- [13] L. J. Klinkenberg, The permeability of porous media to liquids and gases, *Am. Pet. Inst.* **2**, 200 (1941).
- [14] J. Sánchez-Vargas, F. J. Valdés-Parada, and D. Lasseux, Macroscopic model for unsteady generalized Newtonian fluid flow in homogeneous porous media, *J. Non-Newtonian Fluid Mech.* **306**, 104840 (2022).
- [15] E. Skjetne and J.-L. Auriault, Homogenization of wall-slip gas flow through porous media, *Transp. Porous Media* **36**, 293 (1999).
- [16] J. Zinn-Justin, Strong interactions dynamics with Padé approximants, *Phys. Rep.* **1**, 55 (1971).